Liu, Meinan & Xue, Dongfeng (2010) Large-scale fabrication of H2(H2O)Nb2O6 and Nb2O5 hollow microspheres. *Materials Research Bulletin*, *45*(3), p. 333.

Large-scale fabrication of $H_2(H_2O)Nb_2O_6$ and Nb_2O_5 hollow microspheres

Meinan Liu and Dongfeng Xue*

Department of Materials Science and Chemical Engineering, School of Chemical Engineering, Dalian University of Technology, 158 Zhongshan Road, Dalian 116012, P. R. China

**Corresponding author. E-mail: dfxue@chem.dlut.edu.cn*

Abstract

Hollow micro-sized $H_2(H_2O)Nb_2O_6$ spheres constructed by nanocrystallites have been successfully synthesized via a bubble template assisted hydrothermal process. In the reaction process, H_2O_2 acts as a bubble generator and plays a key role in the formation of the hollow structure. An in situ bubble template mechanism has been proposed for the possible formation of the hollow structure. The sphere-like assemblies of these $H_2(H_2O)Nb_2O_6$ nanoparticles have been transformed into their corresponding pseudohexagonal phase Nb_2O_5 through a moderate annealing dehydration process without destroying the hierarchical structure. Optical properties of the as-prepared hollow spheres were investigated. It is exciting that the absorption edge of the hollow Nb_2O_5 microspheres shifts about 18 nm to the violet compared with bulk powders in the UV/vis spectra, indicating its superior optical properties.

Keywords: Hollow structure; Niobium compounds; Solution synthesis

Introduction

In recent years, the fabrication of nano- and micro-structures with hollow interior has attracted much attention because of their attractive characteristics [1]. These hollow materials have various potential applications, including drug delivery, chemical storage, photonic crystals, catalysis, sensors, optoelectronics, and micro-cavity resonance [2,3]. Up to now, many metal oxides with hollow interior have been obtained, such as SnO_2 octahedra [4], TiO_2 spheres [5], VOOH dandelions [6], and ZnO dandelions [7]. In contrast, the synthesis of niobium pentoxide (Nb_2O_5) with various morphologies, especially with hollow structure, remains largely unexplored due to its complexity of crystal nucleation and growth process. Nb_2O_5 is very interesting because its outstanding chemical and physical properties may lead to promising applications in magnetic devices, biotechnology, nanotechnology, and catalysis [8–10]. Particularly, Nb_2O_5 with hollow interior would present a superior performance in capacitor and catalyst. Hence, our strong interest to prepare Nb_2O_5 with hollow interior has been a major motivation for this work.

Recently, a variety of methods have been employed to prepare inorganic materials with hollow interior, for example, spherical silica [11], micro emulsion droplets [12], metal compounds [13], self-assembly techniques [14], and heterophase polymerization process [15]. In most of these methods, templates are usually required to build up hollow architectures, and thus a procedure for removing template is necessary, which would make the synthesis process too complex and probably cause environmental pollution. Therefore, it is desirable to explore a simple and green route for the synthesis of Nb_2O_5 with hollow structure. More recently, a cheap and facile process, the in situ bubble-template process has been used to assemble nanoparticles into hollow structure [7,8]. Herein, we also use this bubble technology to prepare niobium compounds with hollow interior. However, considering the high chemical stability (niobium oxide) and the simple crystal structure of the precursors (niobium halides or niobium alkoxides) [16], it is difficult to construct a well-organized three-dimensional (3D) architecture of niobium compounds in a solution system. Therefore, we designed a novel precursor $H_2(H_2O)Nb_2O_6$, with complex structure and high symmetry to successfully build up niobium compounds with 3D architecture by the simple bubble technology.

In this paper, we synthesized hollow $H_2(H_2O)Nb_2O_6$ spheres via a facile bubble technology combined with hydrothermal route. The spherelike assemblies of these $H_2(H_2O)Nb_2O_6$ nanoparticles have been transformed into their corresponding pseudohexagonal Nb_2O_5 phase through a moderate annealing dehydration process without destroying the hierarchical structure. In addition, a probable formation mechanism for the hollow structure has been proposed and the optical property of these niobium compounds with hollow structure has been studied.

Experimental section

The starting materials, Nb_2O_5 (99.99% purity) and LiOH (A.P.) were used without further purification. In a typical synthesis, fresh niobic acid prepared from 0.5 g Nb_2O_5 (the detailed synthesis processes see Ref. 17) was mixed with 3 mL 28% $NH_3 \cdot H_2O$ and 20 mL 30% H_2O_2 to give a clear and homogeneous solution. LiOH aqueous (0.2 M, 5 mL) was then added to the mixture solution to provide a mild alkaline environment. The prepared solution was transferred into a Teflon-lined stainless steel autoclave of 50 mL capacity and sealed. The reaction was performed at 240 °C for 24 h and then naturally cooled to room temperature. In the post treatment, the white precipitate was centrifuged, to separate the powder from the liquid. It was then washed a few times with deionized water and alcohol and dried at 60 °C for 5 h in air. Finally, the Nb_2O_5 samples were obtained by the calcination of $H_2(H_2O)Nb_2O_6$ in air atmosphere at 500 °C for 2 h.

The morphology and crystal structure of as-synthesized powders were investigated using scanning electron microscopy (SEM, JSM-5600LV, JEOL) and X-ray diffraction (XRD, D/Max 2400, Rigaku) techniques, respectively. The structures of Nb_2O_5 and $H_2(H_2O)Nb_2O_6$ were investigated by Transmission electron microscopy (TEM, Philips, TecnaiG2 20, operated at 200 kV). Thermogravimetric analysis and differential scanning calorimetry (TGA/DSC, SDT Q600, TA) were employed to analyze the thermal behaviors of the synthesized precursor in N_2 atmosphere at a heating rate of 10 °C/min. UV/Vis spectra were obtained using a UV/Vis-NIR spectrophotometer (JASCO, V-570). The infrared spectra (IR) of the prepared niobium compounds were measured by KBr pellet method (using a Nicolet NEXUS infrared spectroscopy) in the range of 400–4000 cm^{-1}.

Results and discussion

XRD pattern of the obtained niobium compound is shown in Fig. 1. It cannot be indexed to any XRD patterns of niobium compounds presented in the Joint Committee on Powder Diffraction Standards (JCPDS) cards or in previous reports, indicating that the synthesized compound may be a new-phased niobium material. However further studying, it can be found that XRD pattern of our samples is almost identical to that of $H_2Ta_2O_6$ (or $H_2(H_2O)Ta_2O_6$) with cubic symmetry, which can well reveal the close resemblance of the crystal structure in these compounds. Furthermore, considering so many similar physical properties between Ta and Nb, the as-obtained niobium compound in this case thus can be reasonably formulated as $H_2Nb_2O_6$ or $H_2(H_2O)Nb_2O_6$.

The structural information of niobium oxide, which was obtained through a moderate annealing dehydration process for $H_2Nb_2O_6$ (or $H_2(H_2O)Nb_2O_6$) at 500 °C for 2 h in air, are also provided by XRD analysis (Fig. 2). A comparison between XRD pattern and the standard card reveals that the powders correspond to TT-Nb_2O_5 phase, possessing a pseudohexagonal structure (JCPDS No. 28-0317). Furthermore, the calculated lattice constants a = 3.612 and c = 3.930 Å are well consistent with the values from the standard card a = 3.607 and c = 3.925 Å (JCPDS No. 28-0317).

For determining the dissociative water content in the obtained compound, the thermostability of the precursor in N_2 atmosphere was studied by means of TGA and DSC (in Fig. 3). The experimental value of the weight loss for the whole H_2O elimination is approximately 19.5% from 50 to 1200 °C. However the weight loss for the dehydration process from $H_2Nb_2O_6$ or $H_2(H_2O)Nb_2O_6$ to Nb_2O_5 is theoretically calculated (see Equations (1) and (2)) to be 6.36% or 11.96%, respectively.

$$H_2Nb_2O_6 \rightarrow Nb_2O_5 + H_2O \tag{1}$$

$$H_2(H_2O)Nb_2O_6 \rightarrow Nb_2O_5 + 2H_2O \tag{2}$$

The experimental value is larger than the theoretical value, which may be caused by the dissociative water molecules attaching on the surface of powders. As shown in the TGA curve, the weight loss can be divided into three stages: the first stage is between 50 and 300 °C; the second one is between 300 and 800 °C; and the third one is between 800 and 1200 °C. Correspondingly, five endothermic peaks are detected, centered at 84, 418, 934, 1024 and 1162 °C, respectively. The first endothermic peak (centered at 84 °C) can be attributed to the volatilization of dissociative water, which is accompanied by a weight loss of approximately 3%. The second one (centered at 418 °C) can be attributed to the dehydration process caused by lattice water in the sample. This stage is accompanied by a weight loss of approximately 14% of the initial weight, which matches well with the calculated value 11.96% from Equation (2), indicating that the synthesized niobium compound is $H_2(H_2O)Nb_2O_6$. It is well known that Nb_2O_5 has various polymorphic forms, i.e., H-phase, M-phase, T-phase, and TT-phase. Among them, H-phase obtained at the highest temperature about 1200

°C is the most thermodynamically stable. Therefore, the rest of three endothermic peaks centered at 934, 1024 and 1162 °C, individually, can be reasonably assigned to the evolution of the phase structure of Nb_2O_5 from T-phase to H-phase. Additionally, XRD result provides the evidence that the samples transform directly to Nb_2O_5 after being heated at 500 °C, as shown in Fig. 2. The absence of other intermediate phase is well consistent with the dehydration process of $H_2(H_2O)Ta_2O_6$ [18]. All these results strongly support the conclusion that the as-obtained niobium compound should be $H_2(H_2O)Nb_2O_6$ in this case.

Fig. 4A shows a typical SEM image of the prepared $H_2(H_2O)Nb_2O_6$ crystallites. It is clearly demonstrated that the crystallites have a uniform spherelike shape with diameter of 1–2 μm. Moreover, some partly broken hollow spheres can be obviously observed. The microstructure of the as-synthesized $H_2(H_2O)Nb_2O_6$ crystallites was further studied by TEM and high magnification TEM (HRTEM). As shown in Fig. 4B, a sharp contrast between the dark edge and pale center definitely indicates the hollow interior. The spheres have a less compact surface and comprise numerous nanoflakes (Fig. 4C). From a HRTEM image, it can clearly observe the extruding nanoflakes on the surface and the thickness of $H_2(H_2O)Nb_2O_6$ shell with 70~100 nm (Fig. 4C). In Fig. 4D, HRTEM image provides further insight into the structures. The HRTEM image recorded on the edge of a flake shows well-defined lattice fringes with interplanar spacing of 0.67 nm for the (111) faces of cubic $H_2(H_2O)Nb_2O_6$, indicating the high crystallinity of this product.

The spherelike assemblies of these $H_2(H_2O)Nb_2O_6$ nanoflakes have been transformed into their corresponding pseudohexagonal phase Nb_2O_5 through a moderate annealing dehydration process without destroying the hierarchical structure (as shown in Fig. 5). The diameter of Nb_2O_5 microspheres is still about 1–2 μm (Figs. 5A–C), and the thickness of the shell is about 100 nm as revealed in the magnified image (Fig. 5C). Nevertheless, the surface of these spheres is relatively denser than that of $H_2(H_2O)Nb_2O_6$ spheres due to the calcination process (as observed in Figs. 5B and C). This hollow Nb_2O_5 microsphere built up from nanoflakes would exhibit promising properties for its application in catalysis, biotechnology, and optical devices.

The H_2O_2 concentration has a great effect on the formation of hollow $H_2(H_2O)Nb_2O_6$ crystallites. When the experiment was carried out with H_2O as the solvent, while keeping other experimental conditions unchanged, products with polyhedral solid structure are obtained (Fig. 6A). $H_2(H_2O)Nb_2O_6$ crystallites have also been prepared at varied H_2O_2 concentration for comparison. The products obtained at a lower H_2O_2 concentration (15%), are composed of a spherelike hollow structure (Fig. 6B), proving that H_2O_2 indeed has a crucial effect on the formation of the hollow structure. The obtained spheres are well dispersive, but the diameter is not uniform, which may be related to the dilute reaction system. As H_2O_2 concentration increases to 30%, the hollow $H_2(H_2O)Nb_2O_6$ microspheres are obtained with uniform diameter, as shown in Fig. 6C. However, the phenomenon of the aggregation is observed, because too many bubbles generates in the reaction system with increasing H_2O_2 concentration. These experimental results prove that H_2O_2 plays a key role in the formation of $H_2(H_2O)Nb_2O_6$ with hollow structure.

Traditionally, the synthesis of Nb_2O_5 involves hydrolyzation of niobium halides or niobium alkoxides [16]. Since these precursors are small molecules, there is no motivation to construct well-organized 3D architectures. As a result, random-arranged nanocrystals are mainly obtained. Therefore, to develop a novel precursor of Nb_2O_5 with complex structure and high symmetry is necessary. We have achieved the aim that $H_2(H_2O)Nb_2O_6$ with cubic structure are obtained via a simple hydrothermal route. As illustrated in Scheme 1, $H_2(H_2O)Nb_2O_6$ can be obtained via two routes: (A) in H_2O system and (B) in H_2O_2/H_2O system. In H_2O system, the obtained $H_2(H_2O)Nb_2O_6$ nanoparticles naturally grow into polyhedra due to its intrinsic crystal habit. However, in H_2O_2/H_2O system, the whole crystalline process and the growth environment of $H_2(H_2O)Nb_2O_6$ have been strongly modified. It should be mentioned that in H_2O_2/H_2O system a chemical reaction among niobic acid, peroxide, and ammonia firstly takes place to form $(NH_4)_3Nb(O_2)_4$ at room temperature [19], as shown in Equation 3. Then this complex decomposes and releases O_2 to form $H_2(H_2O)Nb_2O_6$ (Equation 4) with cubic structure (step I) under hydrothermal condition. The freshly crystalline nanoparticles $H_2(H_2O)Nb_2O_6$ are unstable because of their high surface energy and they tend to aggregate around the gas/liquid interface (O_2/H_2O), driven by the minimization of interfacial energy (step II and III) [6]. As a result, hollow $H_2(H_2O)Nb_2O_6$ microspheres are formed, which are constructed by numerous nanoparticles. Finally, the Nb_2O_5 hollow microspheres are obtained through the simple pyrolysis of its precursor $H_2(H_2O)Nb_2O_6$ in air atmosphere without destroying the hierarchical structure (step IV). The effect of H_2O_2 should be highlighted due to its importance in the formation of the hollow structure. In the reaction system, it acts not only as the coordination reagent but also as the bubble generator. Furthermore, the experimental results of the influence of H_2O_2 concentration also support this proposed mechanism.

$$Nb_2O_5{\cdot}nH_2O + 6NH_3{\cdot}H_2O + 9H_2O_2 \rightarrow 2(NH_4)_3Nb(O_2)_4 + (12+n)H_2O + O_2 \quad (3)$$

$$2(NH_4)_3Nb(O_2)_4 + 5H_2O \rightarrow H_2(H_2O)Nb_2O_6 + 6NH_4OH + 4O_2 \quad (4)$$

To evaluate the optical properties of the obtained samples with hollow interior structure, the UV/vis spectra of $H_2(H_2O)Nb_2O_6$ and Nb_2O_5 are illustrated in Fig. 7. In comparison, we also characterized the UV/vis spectra of the bulk Nb_2O_5 powders. As shown in the spectra, two major absorption bands for bulk Nb_2O_5 with maxima appear at about 220 and 308 nm (Fig. 7), respectively. The absorption band above 300 nm corresponds to the band gap of the corner-sharing NbO_6 octahedra, while the band at 220 nm is from the NbO_6 octahedra with other configurations, for instance, edge-sharing octahedra [20]. It is exciting that the absorption edge of the hollow Nb_2O_5 microspheres shifts 18 nm to the violet compared to that of bulk Nb_2O_5. That is caused by the quantum size effect from those nanocrystallites on the surface of the microspheres and the thin shell (thickness smaller than 100 nm). Interestingly, the absorption edge of the obtained $H_2(H_2O)Nb_2O_6$ shifts further to the violet, which may be caused by the effect of H atom in the structure on the electro cloud of O_{2p}. As the UV results shown, these hollow microspheres are expected to exhibit superior optical properties due to their unique hollow structure and large internal surface area at their interior.

Conclusion

New-phased $H_2(H_2O)Nb_2O_6$ and pseudohexagonal phase Nb_2O_5 with hollow interior have been successfully synthesized, for the first time, via a simple bubble template route combined with hydrothermal process. The experimental results showed that H_2O_2 plays a key role in the formation of hollow spheres. The as-obtained hollow $H_2(H_2O)Nb_2O_6$ microspheres presents high crystallinity and exhibits superior optical properties, which may be expected to be a promising candidate for both fundamental research and functional applications. Furthermore, comparing to the bulk Nb_2O_5, the evident violet shift of the absorption edge well indicates the outstanding optical properties of the obtained Nb_2O_5 microsphere due to its novel 3D architecture. We believe that the hollow Nb_2O_5 microsphere will remarkably promote its special performances in terms of catalysis, drug-carrier, and gas sensors.

Acknowledgements:

The financial support from Program for the National Natural Science Foundation of China (Grant No. 50872016) is greatly acknowledged.

References

[1] Z. W. Shan, G. Adesso, A. Cabot, M. P. Sherburne, S. A. S. Asif, O. L. Warren, D. C. Chrzan, A. M. Minor, A. P. Alivisatos, Nature Mater. 7 (2008) 947.

[2] Y. Piao, J. Kim, H. B. Na, D. Kim, J. S. Baek, M. K. Ko, J. H. Lee, M. Shokouhimehr, T. Hyeon, Nature Mater. 7 (2008) 242.

[3] D. Grosso, C. Boissiere, C. Sanchez, Nature Mater. 6 (2007) 572.

[4] H. G.Yang, H. C. Zeng, Angew. Chem. Int. Ed. 43 (2004) 5930.

[5] X. Li, Y. Xiong, Z. Li, Y. Xie, Inorg. Chem.45 (2006) 3493.

[6] C. Wu, Y. Xie, L. Lei, S. Hu, C. Yang, Adv. Mater. 18 (2006) 1727.

[7] B. Liu, H. C. Zeng, J. Am. Chem. Soc. 126 (2004) 16744.

[8] P. Yang, D. Zhao, D. Margolese, B. Chmelka, G. Stucky, Nature 396 (1998) 152.

[9] (a) Z. Huo, C. Tsung, W. Huang, M. Fardy, R. Yan, X. Zhang, Y. Li, P. Yang, Nano Lett. 9 (2009) 1260. (b) L. Li, J. Deng, J. Chen, X. Sun, R. Yu, G. Liu, X. Xing, Chem. Mater. 21 (2009) 1207.

[10] (a) S. Guerrero, J. T. Miller, A. J. Kropf, E. E. Wolf, J. Catal. 262 (2009) 102. (b) M. Ziolek, Catal. Today 78 (2003) 47. (c) K. Tanabe, Catal. Today 78 (2003) 65.

[11] J. S. Jan, S. Lee, C. S. Carr, D. F. Shantz, Chem. Mater. 17 (2005) 4310.

[12] J. Wang, Y. Xia, W. Wang, R. Mokaya, M. Poliakoff, Chem. Commun. (2005) 210.

[13] (a) C. Yan, D. Xue, J. Phys. Chem. B 110 (2006) 11076. (b) C. Yan, D. Xue, J. Phys. Chem. B 110 (2006) 7102.

[14] J. Hu, L. Ren, Y. Guo, H. Liang, A. Cao, L. Wan, C. Bai, Angew. Chem. Int. Ed. 44 (2005) 1269.

[15] (a) Q. Sun, Y. Deng, J. Am. Chem. Soc. 127 (2005) 8274. (b) X. H. Li, D. H. Zhang, J. S. Chen, J. Am. Chem. Soc. 128 (2006) 8382.

[16] (a) N. Pinna, M. Antonietti, M. Niederberger, Colloids and Surfaces A 250 (2004) 211. (b) M. Ristic, S. Popovic, S. Music, Mater. Lett. 58 (2004) 2658. (c) P. R. Bueno, C. O. Avellaneda, R. C. Faria, L. O. S. Bulhoes, Electrochim. Acta 46 (2001) 2113.

[17] M. Liu, D. Xue, C. Luo, J. Am. Ceram. Soc. 89 (2006) 1551.

[18] (a) M. Hervieu, C. Michel, B. Raveau, Bull. Soc. Chim. Fr. 11 (1971) 3939. (b) D. Groult, J. Pannetier, B. Raveau, J. Solid State Chem. 41 (1982) 277.

[19] D. Bayot, B. Tinant, M. Devillers, Catal. Today 78 (2003) 439.

[20] M. Liu, D. Xue, J. Phys. Chem. C 112 (2008) 6346.

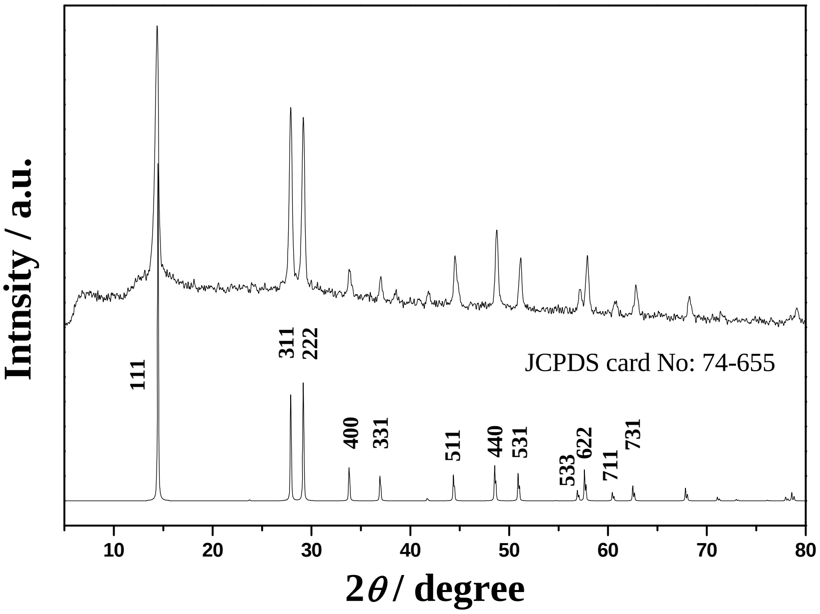

Fig. 1. XRD pattern of the sample $H_2(H_2O)Nb_2O_6$ and the standard diffraction pattern of $H_2(H_2O)Ta_2O_6$ (JCPDS No. 74-655) shown as a reference.

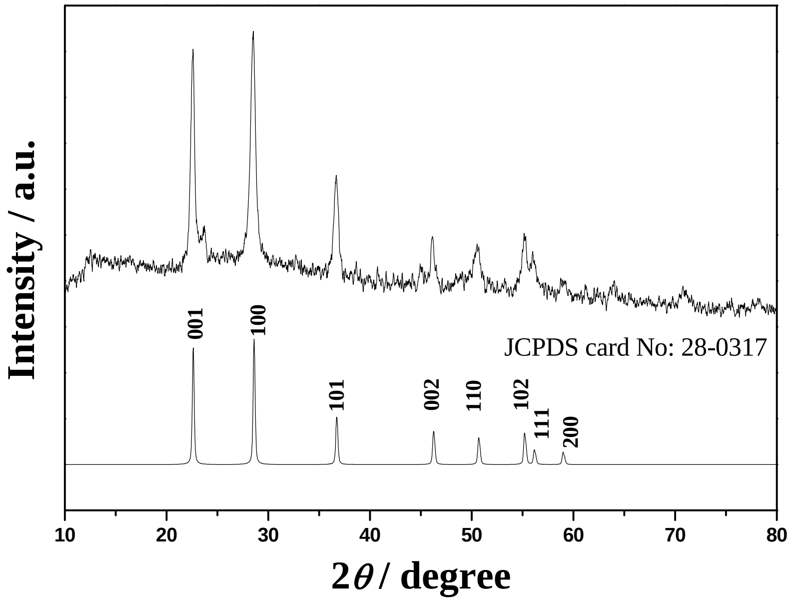

Fig. 2. XRD pattern of Nb_2O_5 obtained by heating its precursor $H_2(H_2O)Nb_2O_6$ in air atmosphere at 500 °C for 2 h. Moreover the standard diffraction pattern of Nb_2O_5 (JCPDS No. 28-0317) is shown as a reference.

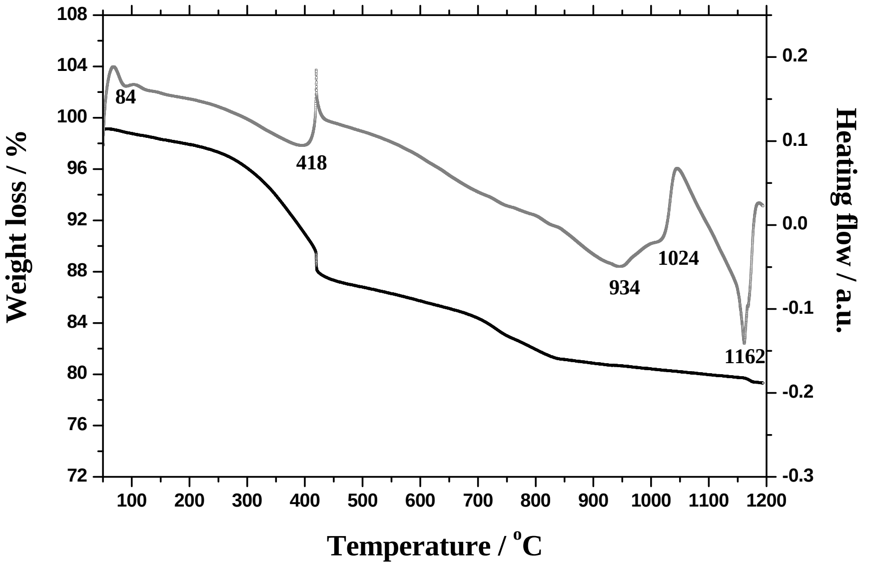

Fig. 3. Typical TGA and DSC curves of as-obtained $H_2(H_2O)Nb_2O_6$ hollow microspheres measured at a heating rate of 10 °C/min in N_2 atmosphere.

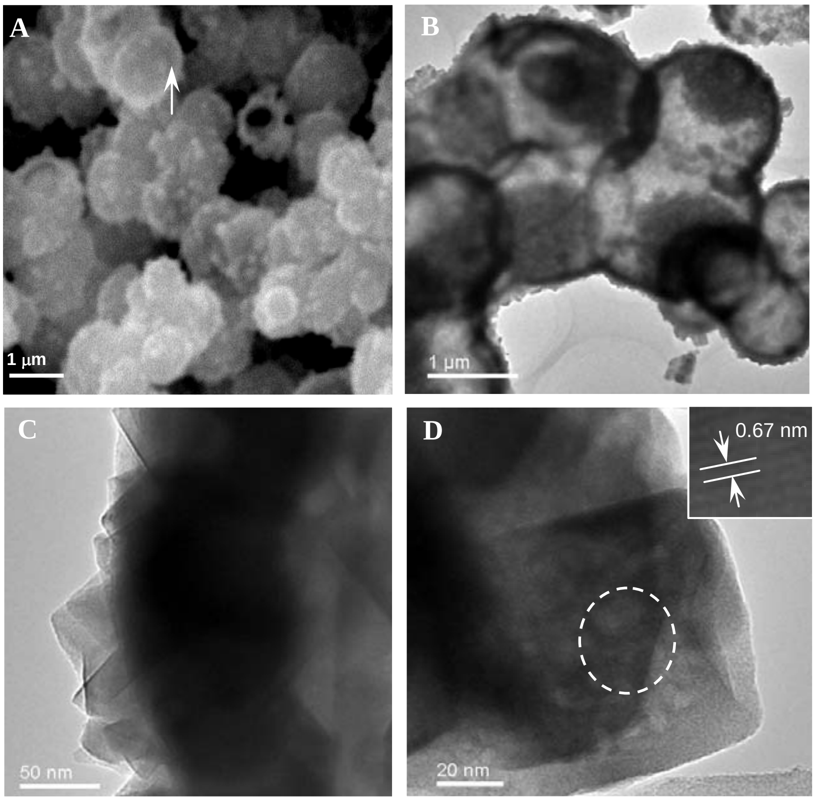

Fig. 4. A) Typical SEM image of the as-prepared $H_2(H_2O)Nb_2O_6$ sample. B–D) Typical TEM images of the product. Inset D shows HRTEM image recorded on the edge of a nanoflake as delineated by the white circle in D.

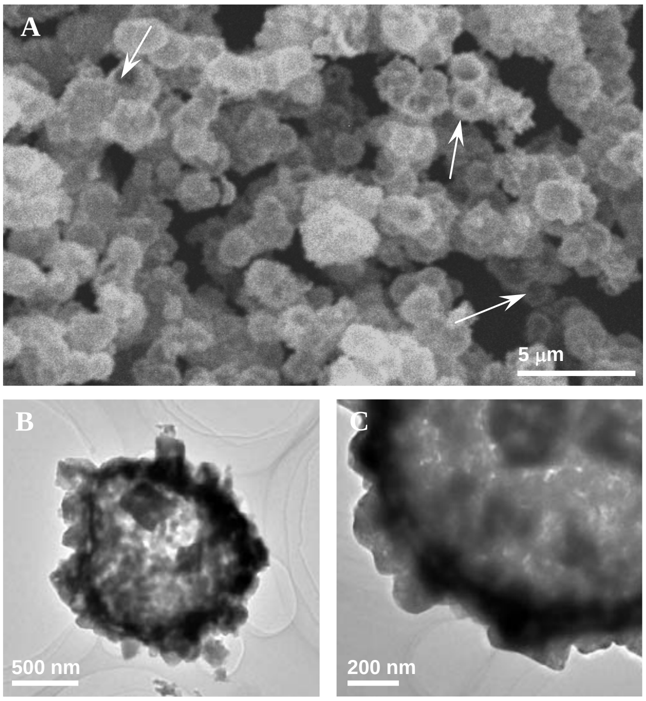

Fig. 5. Typical SEM image A and TEM images (B and C) of Nb_2O_5 hollow microspheres obtained by the calcination of its precursor $H_2(H_2O)Nb_2O_6$ in air atmosphere at 500 °C for 2 h. These arrows are drawn as a guide to the eyes.

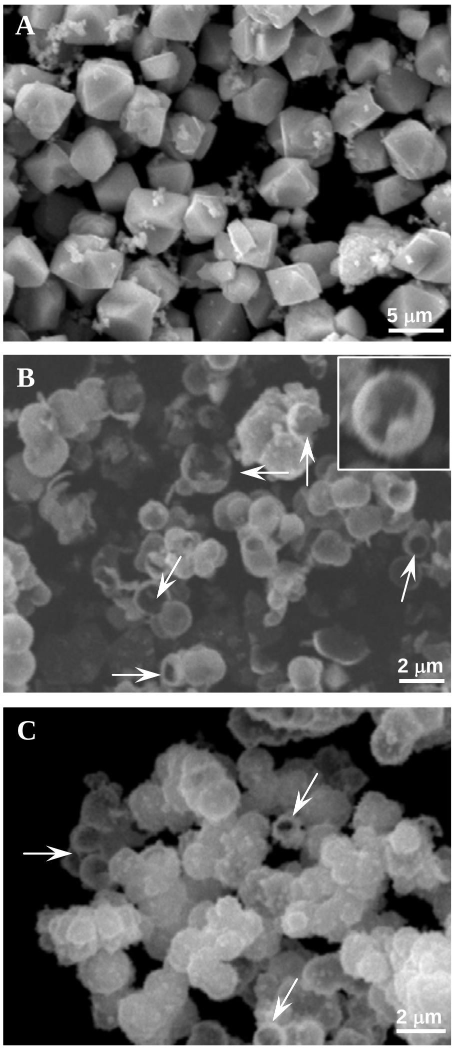

Fig. 6. Typical SEM images of $H_2(H_2O)Nb_2O_6$ samples prepared in hydrothermal system: (A) without H_2O_2 and (B, C) under different H_2O_2 concentrations; (B) 15%, (C) 30%. Inset B shows a typical broken sphere and these arrows are drawn as a guide to the eyes.

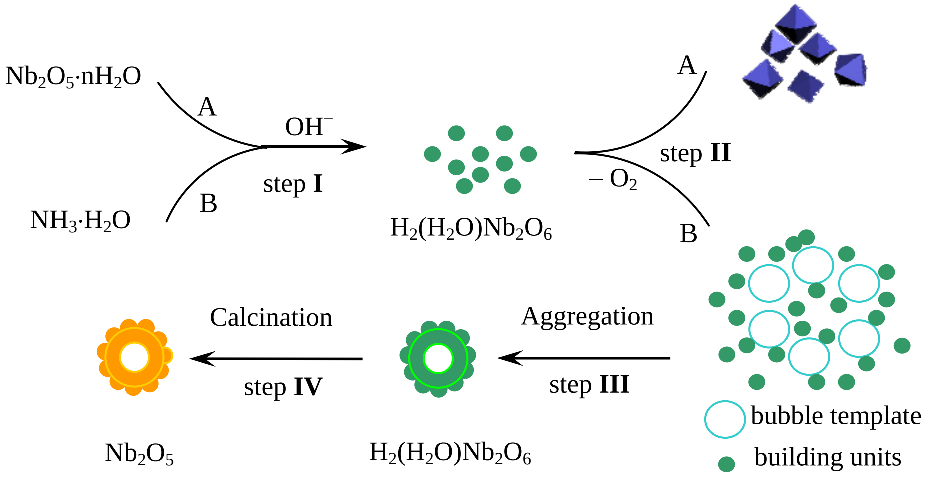

Scheme 1. Schematic illustration of the evolution of $H_2(H_2O)Nb_2O_6$ prepared via two routes: (A) in H_2O system; (B) in H_2O_2/H_2O system, and Nb_2O_5 hollow microspheres.

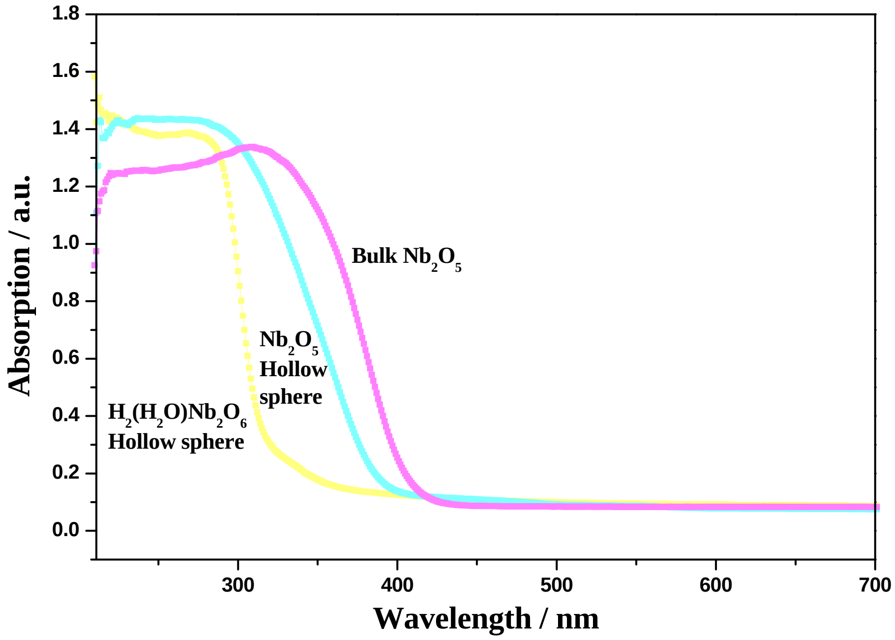

Fig. 7. UV/Vis spectra of as-obtained $H_2(H_2O)Nb_2O_6$ hollow microspheres, Nb_2O_5 hollow microspheres, and bulk Nb_2O_5 powders.